Electronic structure of Bi_2X_3 (X=S, Se, T) compounds: Comparison of theoretical calculations with photoemission studies

P. Larson, V. A. Greanya, W. C. Tonjes, Rong Liu, and S. D. Mahanti
Department of Physics & Astronomy, Michigan State University, East Lansing, Michigan 48824

C. G. Olson
Ames Laboratory, Ames, Iowa 50010

(Received 22 February 2001; revised manuscript received 28 September 2001; published 8 February 2002)

In recent years electronic structures of Bi_2Te_3 and related materials have been studied theoretically through *ab initio* band-structure calculations and experimentally through photoemission experiments, but to the best of our knowledge, a detailed comparison between experiment and theory has not been attempted so far. In this paper we discuss the density of states (DOS) of the narrow-gap semiconductors Bi_2X_3 (X=S, Se, Te) obtained within density-functional theory. While several electronic structure calculations for Bi_2Te_3 and Bi_2Se_3 have been reported in the literature, there have been no published calculations for Bi_2S_3 or Bi_2Te_2Se. Recent photoemission and inverse-photoemission measurements in these systems, performed by four separate groups (including our photoemission measurements of Bi_2Te_3 and Bi_2Se_3), allows for a comparison of the general features of the calculated DOS for both valence- and conduction-band states with photoemission and inverse-photoemission spectra. The agreement between the positions of the prominent peaks in the calculated DOS and photoemission spectra continues to improve with better energy resolution in the experiment.

DOI: 10.1103/PhysRevB.65.085108 PACS number(s): 71.20.Nr, 79.60.−i, 72.20.Pa

I. INTRODUCTION

Bi_2X_3 (X=S, Se, Te) belongs to a class of compounds that has been of great interest for its technological applications.[1] In particular, Bi_2Te_3 and its alloys with Sb_2Te_3 and Bi_2Se_3 have been used extensively in room-temperature thermoelectric applications for more than 30 years due to their large figure of merit.[2] Bi_2S_3 has an electrical conductivity that is too small for thermoelectric applications,[3] but it has been investigated as a potential material for photovoltaic converters.[4] While careful and extensive electronic structure calculations have been made for Bi_2Se_3 (Refs. 5 and 6) and Bi_2Te_3 (Refs. 6–8), electronic structure calculations for Bi_2Te_2Se and Bi_2S_3, the latter forming in a different crystal structure, have not, to the best of our knowledge, been performed.

Previous electronic structure calculations have compared the band gaps and effective masses of Bi_2Te_3 to experiment.[6,8] These properties rely on understanding the band structure to within ~0.1 eV of the Fermi energy. However, the calculated band structures have not been tested over a larger energy scale. Photoemission (PES) and inverse-photoemission (IPES) studies, on the other hand, allow for a comparison of the calculated band structure (using angle-resolved PES and IPES) and density of states (using angle-integrated PES and IPES) over a much larger energy range (~10 eV).[9] Angle-integrated PES measures the joint density of states of the initial and final states modified by the matrix element. At high photon energies ($h\nu > 100$ eV), the final state is nearly free-electron-like and the measured spectra can be identified approximately with the DOS of the initial state, modified by the matrix element between an initial atomiclike and final plane-wave state. Since we are interested in a range of energy of about 10 eV or less, we do not expect a strong energy dependence of the matrix element in this range at such high photon energies and the PES spectra can be directly compared with the occupied DOS. However, PES experiments at high photon energy tend to have poor energy resolution. Higher-energy resolution (better than 0.1 eV) can be achieved at lower photon energies. In the latter case, the energy dependence of the matrix element and the final-state DOS can become important. Thus, a direct comparison of the details of the energy dependence of the calculated DOS of the occupied states and the measured spectra is not very meaningful. However, a comparison of the general features such as the valence-band width, number of prominent peaks, and the peak positions is still a useful test of the electronic structure calculations.

In this paper we compare the electronic structures of four systems, Bi_2S_3, Bi_2Se_3, Bi_2Te_2Se, and Bi_2Te_3, obtained using *ab initio* methods, with earlier PES and IPES experiments[10–12] and our PES study. High-resolution angle-integrated PES experiments were performed on Bi_2Se_3 and Bi_2Te_3 using multiple photon energies. We find that improvements in the energy resolution and carrying out PES measurements at different incident photon energies lead to more distinguishable peaks in the photoemission spectra, which are in better agreement with the calculated DOS.

This paper is organized as follows: In Sec. II the method and results of the electronic structure calculations will be discussed briefly. Section III describes the experimental method with an analysis of the current photoemission results. The results of these photoemission studies are then compared with the calculated DOS in Sec. IV. Section V follows with a summary and conclusions.

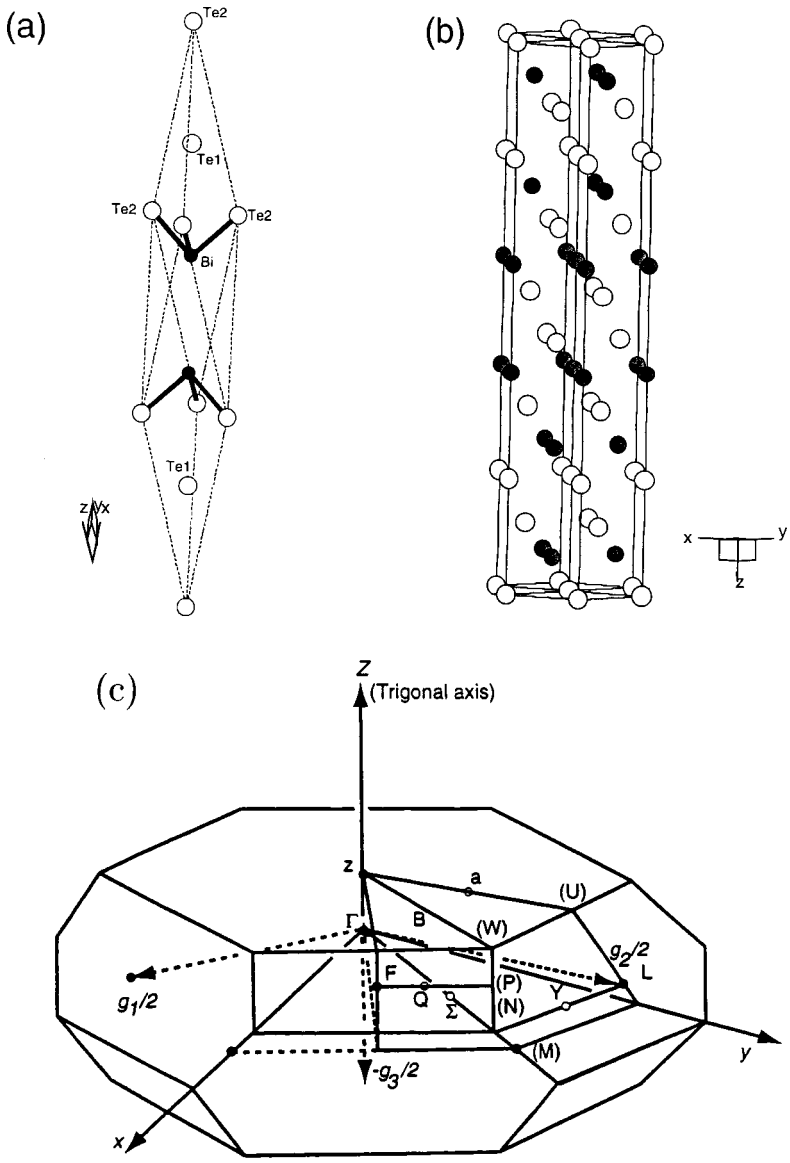

FIG. 1. (a) Rhombohedral unit cell (b) hexagonal unit cell, and (c) rhombohedral Brillouin zone of Bi_2Se_3, Bi_2Te_2Se, and Bi_2Te_3. The crystal structure of Bi_2Te_3 is shown. In Bi_2Se_3 the Te atoms are replaced by Se atoms, while in Bi_2Te_2Se the Te1 position remains unchanged while the atoms at the Te2 positions are replaced by Se.

II. THEORETICAL CALCULATIONS

A. Method of calculations

Electronic structure calculations were performed using the self-consistent full-potential linearized augmented plane-wave method (FLAPW) (Ref. 13) within density-functional theory (DFT).[14] The generalized gradient approximation (GGA) of Perdew, Burke, and Ernzerhof[15] was used for the exchange and correlation potentials. Calculations were performed using the WIEN97 package.[16] Values of the atomic radii were chosen to fill the space between the atoms. The values are 2.0 a.u. for Bi and S in Bi_2S_3, 2.8 a.u. for Bi and Se in Bi_2Se_3, 2.86 a.u. for Bi, Te, and Se in Bi_2Te_2Se, and 2.9 a.u. for Bi and Te in Bi_2Te_3, where a.u. is the atomic unit (0.52 A). Adjustments of these parameters within a reasonable range showed little dependence on this variation. Self-consistent iterations were performed for 44 **k** points for Bi_2Se_3, Bi_2Te_2Se, and Bi_2Te_3 and 20 **k** points for Bi_2S_3 inside the reduced Brillouin zone. The convergence in energy was within 0.0001 Ry with RK_{MAX} chosen as 8 and G_{MAX} chosen as 10 $bohr^{-1}$. Scalar relativistic corrections were added for all systems studied and spin-orbit interaction was incorporated using a second variational procedure.[17]

B. Bi_2Se_3, Bi_2Te_2Se, and Bi_2Te_3

The crystal structure of Bi_2Se_3, Bi_2Te_2Se, and Bi_2Te_3 is rhombohedral with the space group D_{3d}^5 ($R\bar{3}m$) containing five atoms in the unit cell.[18] The rhombohedral unit cell along with the hexagonal unit cell are given in Figs. 1(a) and 1(b), respectively. The Brillouin zone (BZ) for the rhombohedral cell is given in Fig. 1(c). Along the *z* direction (trigonal axis) these compounds consist of five-atom layers (referred to as "quintuple layer leaves") with primarily strong ionic and covalent bonding within the layers, and weak van der Waals bonding between the layers.[6,8,19] The five atoms inside a unit cell reduce to three inequivalent atoms identified as Te1 (Te1/Se1), Te2 (Se2/Se2), and Bi as shown in Fig. 1(a) for Bi_2Te_3 (Bi_2Te_2Se/Bi_2Se_3). The lattice parameters *a* and *c* of the hexagonal unit cell are in (Å) 4.138 and 28.64,

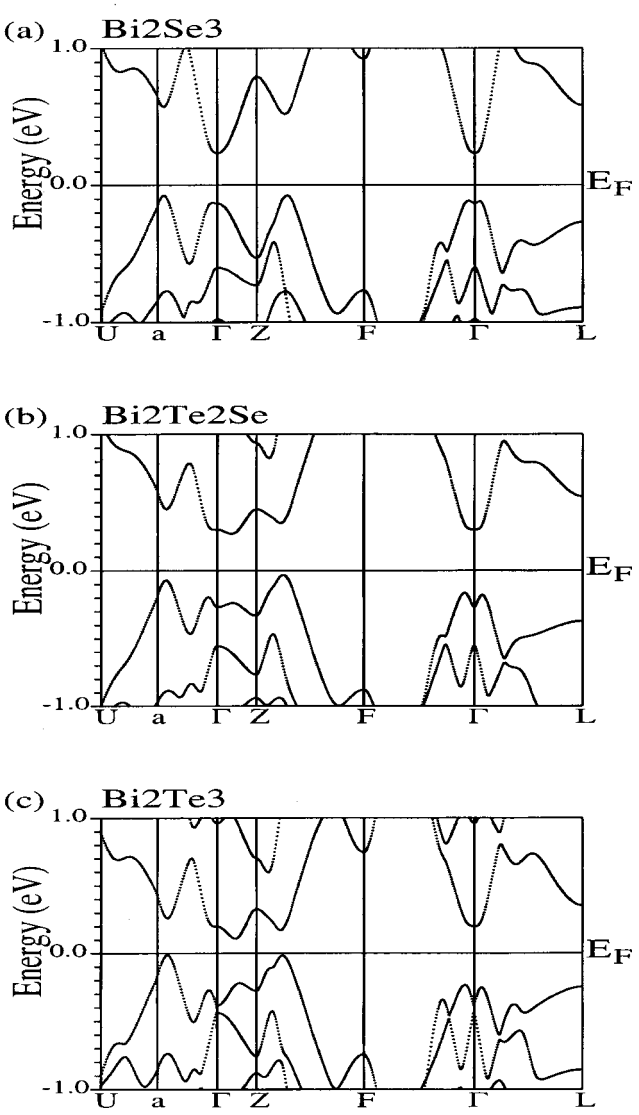

FIG. 2. Band structures of (a) Bi_2Se_3, (b) Bi_2Te_2Se, and (c) Bi_2Te_3. The zero of energy lies within the semiconducting gap.

4.28 and 29.86, and 4.38 and 30.487 for Bi_2Se_3, Bi_2Te_2Se, and Bi_2Te_3, respectively. These parameters and the atomic positions were taken from Wyckoff.[18]

In earlier calculations,[6–8] spin-orbit interaction was found to significantly affect the band structure of Bi_2Te_3. We will therefore discuss the results of band-structure calculations for Bi_2Se_3, Bi_2Te_2Se, and Bi_2Te_3 including spin-orbit interaction. We find (see Fig. 2) that the valence-band maxima in all three compounds occur along ZF and $Ua\Gamma$ with a nearly equivalent peak at the Γ point in Bi_2Se_3. The conduction-band minima occurs along ΓZ. Bi_2Te_2Se, like Bi_2Te_3, is an indirect-gap semiconductor with a band gap 0.33 eV (in Bi_2Te_3 the band gap is 0.17 eV). In contrast, Bi_2Se_3 is a direct-gap semiconductor with a band gap 0.32 eV. Since our results for Bi_2Te_3 have been discussed in detail previously,[8] we will refer to this paper for our major findings in this system.

Our electronic structure calculation for Bi_2Se_3 agrees well on a broad scale with the previous linear muffin-tin orbital within the atomic sphere approximation (LMTO-ASA) calculation,[6] but neither of these two calculations agree with the earlier pseudopotential results.[5] The linearized augmented plane-wave (LAPW)-GGA calculation gives a band gap of 0.32 eV, slightly larger than 0.24 eV found by Mishra, Satpathy, and Jepsen.[6] However both are close to the experimental value, which lies in the range 0.2–0.3 eV.[20] The main difference between LAPW-GGA and LMTO-ASA calculations appears to be that in the former the valence-band peak at the Γ point has nearly the same energy as the two secondary peaks, whereas this peak was found to have a higher energy in the LMTO-ASA calculation.[6] In fact, in our calculation what appears to be a peak in the valence band at the Γ point is really a saddle point with a maximum only along the ΓZ direction. While electron-doped Bi_2Se_3 is known to have one minimum at the Γ point, in agreement with theoretical calculations, the hole-doped Bi_2Se_3 has not yet been produced and therefore has not yet been studied experimentally.[21,22] We find two sixfold-degenerate hole pockets at general points of the BZ and one saddle surface near the Γ point. It will be interesting to check these theoretical predictions experimentally.

Unlike Bi_2Te_3 (Refs. 6–8 and 24) and Bi_2Se_3,[20–22] to the best of our knowledge, there has been no theoretical or experimental analysis of the band gap in Bi_2Te_2Se. The unit cell of this compound differs from that of Bi_2Te_3 by replacing one Te atom by a Se atom, the Se atom going into the Te2 site[23] [Fig. 1(a)]. The electronic structure of Bi_2Te_2Se closely resembles that of Bi_2Te_3. The top of the valence band forms along $Ua\Gamma$ and ZF, while the bottom of the conduction band forms along ΓZ. While Bi $6p$ states are mostly above E_F and Te1 $5p$ states are mostly below E_F, a strong hybridization of the Bi $6p$ and Te1 $5p$ occurs along ΓZ, similar to what is seen in Bi_2Te_3.[8] The Se2 $4p$ states do not appear to play any significant role near E_F, similar to what was found for Te2 $5p$ states in Bi_2Te_3.[8] In Bi_2Se_2Te, where the roles of Te and Se atoms are interchanged, the band structure is found to closely resemble that of Bi_2Se_3 with a direct gap at the Γ point.

C. Bi_2S_3

Although S lies in the same column in the Periodic Table as Se and Te, Bi_2S_3 forms in a different crystal structure than Bi_2Se_3 and Bi_2Te_3. The crystal structure of Bi_2S_3 is orthorhombic in the space group V_h^{16} (*Pbnm*) with twenty atoms in the unit cell.[18] The orthorhombic unit cell and its corresponding Brillouin zone are shown next to each other in Figs. 3(a) and 3(b), respectively. The crystal structure consists of sheets of atoms parallel to the z axis with each S surrounded by three Bi atoms and each Bi atom surrounded by three S atoms.[18] These 20 atoms reduce to five inequivalent atoms identified as Bi1, Bi2, S1, S2, and S3 in Fig. 3(a). The lattice parameters ($a-c$) are 11.15, 11.30, and 3.981 A. These and the atomic positions were taken from Wyckoff.[18]

Electronic structure calculations for Bi_2S_3 show a semiconductor with a large number of bands within a few eV of E_F. The top of the valence band and the bottom of the conduction band both lie at general points along ΓX to form a

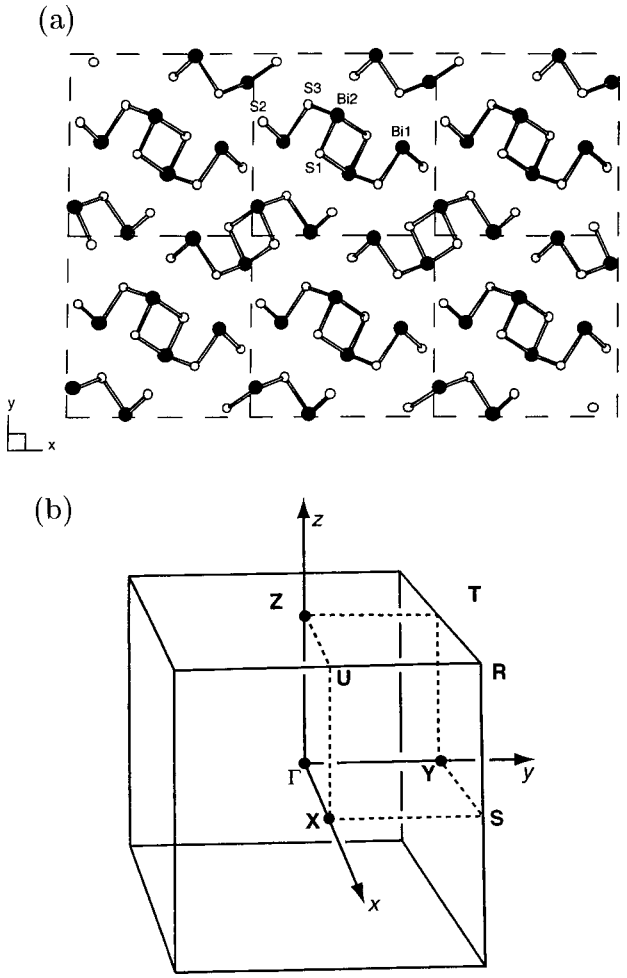

FIG. 3. (a) Orthorhombic unit cell of Bi_2S_3 (shown in the a-b plane) and its corresponding (b) Brillouin zone.

nearly direct gap of 1.24 eV (Fig. 4). The band gap has been measured by several groups to be between 1.2–1.7 eV,[3,25] one of the most recent measurements giving a value of 1.3 eV.[3]

In order to better understand the electronic structure of this material near the gap region, an orbital analysis of the bands near E_F was performed. We find that Bi1 and Bi2 6p orbitals contribute primarily to the bottom of the conduction band while S1, S2, and S3 3p orbitals contribute to the top of the valence band. There is some hybridization between these orbitals, but significantly less than the hybridization between the Bi 6p and Te1 5p orbitals in Bi_2Te_3.[6,8] Thus Bi_2S_3 is more ionic. These differences between Bi_2S_3, and Bi_2Te_3 and Bi_2Se_3 can be ascribed to (i) the different crystal structure of Bi_2S_3 compared to Bi_2Te_3 and Bi_2Se_3 and (ii) different electronic affinities of S, Se, and Te. The general features of the band structure over a broader energy range will be discussed in Sec. IV after discussing the results of photoemission measurements.

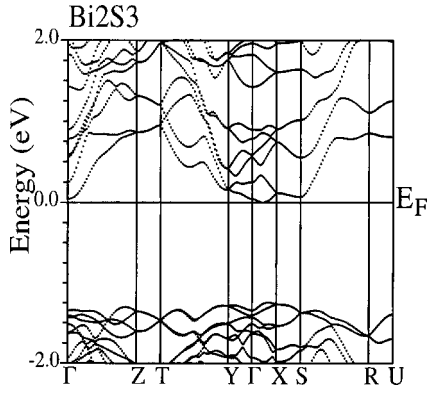

FIG. 4. Band structures of Bi_2S_3. The zero of energy lies within the semiconducting gap.

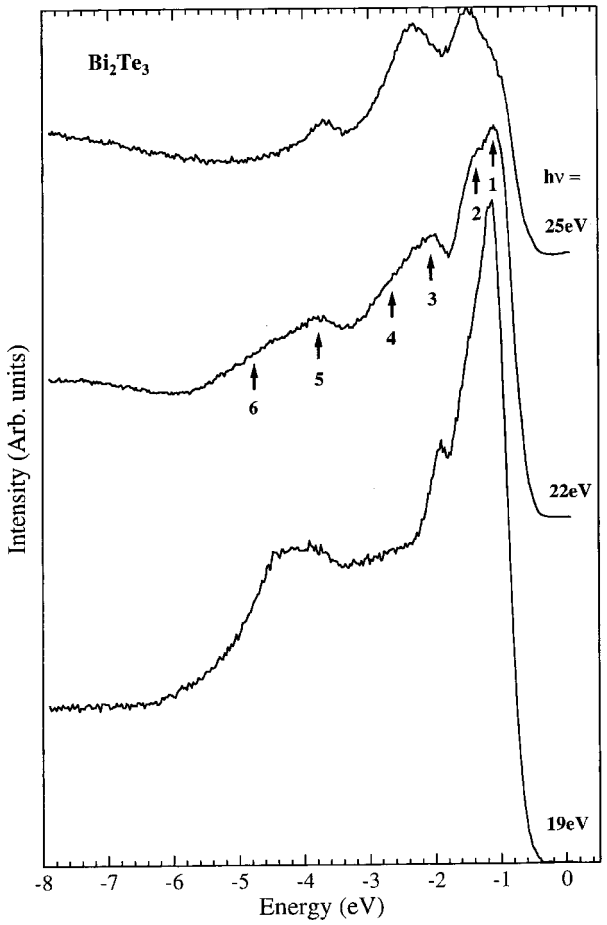

FIG. 5. Present photoemission spectrum for Bi_2Te_3. Peaks 1–6 are indicated by arrows. For the purpose of comparison, the energy reference (zero of energy) was set such that the lowest binding-energy peak in the spectra coincides with the position of the corresponding peak in the data from the previous UPS experiment by Ueda *et al.* (Ref. 11).

III. PHOTOEMISSION EXPERIMENTS

We will now discuss the results of our angle-integrated PES measurements in p-type Bi_2Te_3 and n-type Bi_2Se_3 single crystals. These single crystals were grown by slow cooling a molten Bi/Te(Se) mixture. The p-type Bi_2Te_3 was prepared with additional Bi as a dopant, which substitutes for Te atoms in the crystal lattice. On the other hand the Bi/Se

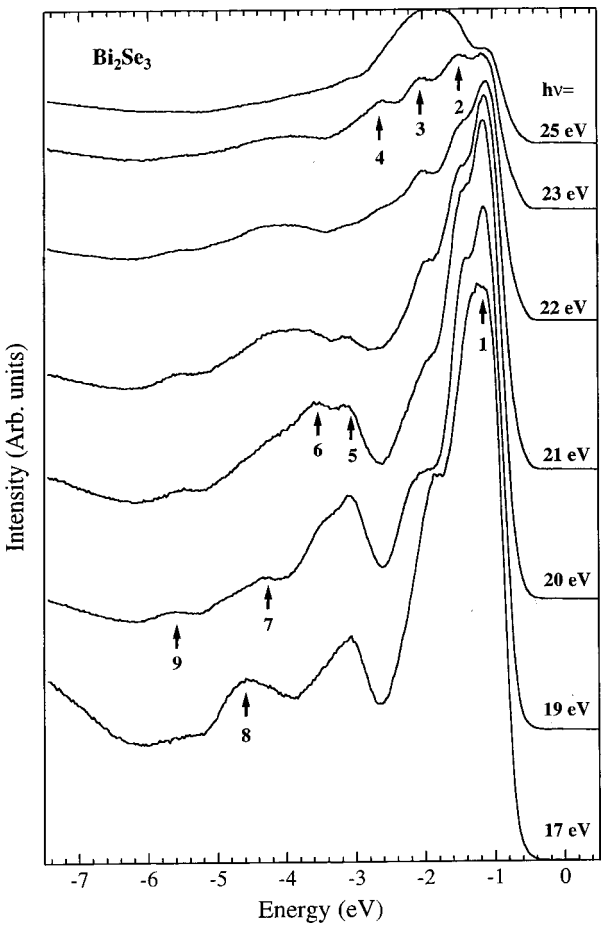

FIG. 6. Present photoemission spectrum for Bi_2Se_3. Peaks 1–9 are indicated by arrows. For the purpose of comparison, the energy reference (zero of energy) was set such that the lowest binding-energy peak in the spectra coincides with the position of the corresponding peak in the data from the previous UPS experiment by Ueda *et al.* (Ref. 11).

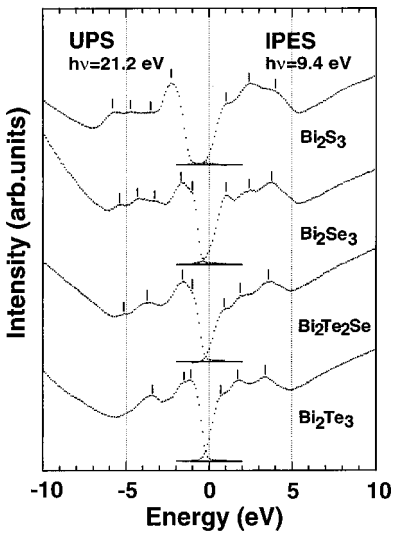

FIG. 7. Valence-band photoemission (UPS) and conduction-band inverse-photoemission (IPES) for Bi_2S_3, Bi_2Se_3, Bi_2Te_2Se, and Bi_2Te_3 crystals. UPS and IPES spectra for each crystal are connected at E_F. Energies are referred to E_F (courtesy of Yoshifumi Ueda) (Ref. 11).

melt always results in *n*-type Bi_2Se_3. Thermopower measurements in these samples indicated the type of doping. PES measurements were carried out at the Synchrotron Radiation Center in Stoughton, Wisconsin, on the Ames-Montana ERG-Seya beam line. A double-pass cylindrical mirror analyzer was used. The energy resolution was 0.08 eV for all spectra. The crystals were cleaved in an ultrahigh vacuum ($\sim 1\times 10^{-10}$ Torr) to obtain clean surfaces. Spectra were taken at room temperature.

Figures 5 and 6 show the angle-integrated PES spectra of Bi_2Te_3 and Bi_2Se_3, respectively, taken at multiple photon energies as indicated. For the purpose of comparison with the earlier PES experiments by Ueda *et al.*[11] and with the theoretical DOS, the energy reference was set such that the lowest binding-energy valence-band peaks in both Bi_2Te_3 and Bi_2Se_3 spectra coincided with the corresponding peaks in the data from Ueda *et al.*[11]

As can be seen in these figures, the spectra for both Bi_2Te_3 and Bi_2Se_3 show dramatic changes in the shape as the photon energy is varied, indicating strong matrix element effects. Some features are more prominent and are easier to identify at certain photon energies than others. For Bi_2Te_3 the spectra at 22 eV seems to show the most number of prominent features. Six features, labeled 1 through 6, are identified. While feature 1 in the 22-eV spectrum is quite prominent, it appears only as a shoulder in the 25-eV spectrum. Also, the separation between features 1 and 2 is not as obvious in the 19-eV spectrum. Peak 6 is barely visible in the 25-eV spectrum, and peak 4 is not obvious in the 19- and 25-eV spectra. Also, the apparent peak positions of features 3 and 5 appear to have shifted slightly (by $\sim$0.2–0.3 eV) in the 25-eV spectrum. This illustrates that, when studying the valence-band electronic structure with low photon energies, it is important to measure spectra at multiple photon energies. A spectrum measured at a single photon energy is not as informative and may even be misleading.

For Bi_2Se_3 (Fig. 6) a large number of features can be identified in the spectra. Nine features, labeled 1 through 9, are identified in the spectra measured with various photon energies. Again, some features are more easily identifiable at certain photon energies than others and the apparent peak positions might show small shifts due to matrix element effects.

Several groups have performed angle-integrated PES experiments on these systems previously. Debies and Rabalais[10] studied Bi_2O_3, Bi_2S_3, Bi_2Se_3, and Bi_2Te_3 using Al $K\alpha$ radiation (1486.6 eV) with an unspecified energy resolution. Nascimento *et al.*[12] studied Bi_2Se_3 also using Al $K\alpha$ radiation with an energy resolution of 0.8 eV. In both studies, the spectra show only a couple of broad spectral features. In a more recent study, Ueda *et al.*[11] studied Bi_2S_3, Bi_2Se_3, Bi_2Te_2Se, and Bi_2Te_3 using both PES and IPES (Fig. 7). In their PES experiments, spectra were measured at $h\nu=21.2$ eV using a helium lamp. The energy resolution was 0.2 eV. While their spectra on Bi_2Te_3 and Bi_2Se_3 show more details than those of Debies and Rabalais[10] and Nasci-

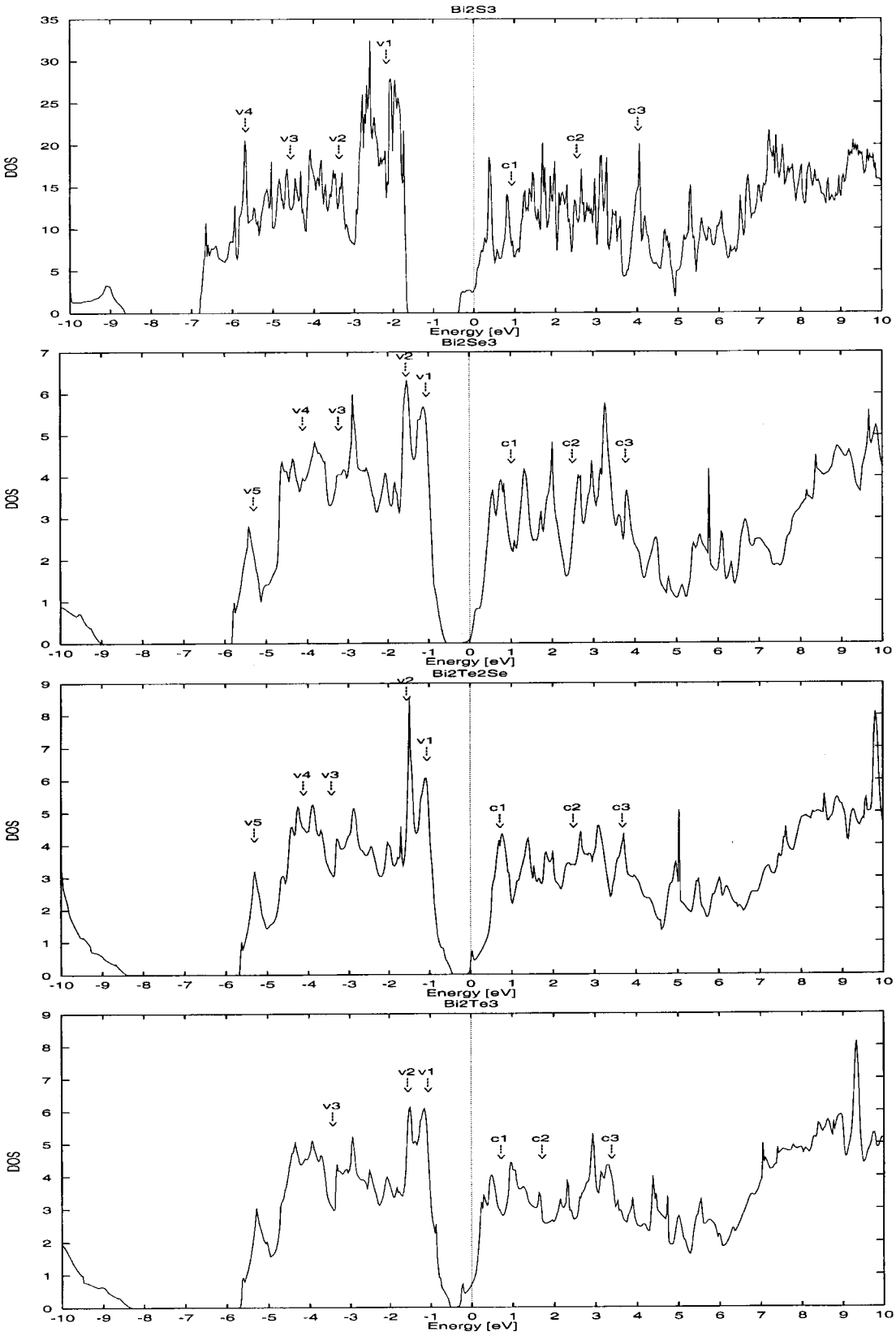

FIG. 8. Total density of states of (a) Bi_2S_3, (b) Bi_2Se_3, (c) Bi_2Te_2Se, and (d) Bi_2Te_3. The arrows indicate the positions of the photoemission peaks seen in the work of Ueda *et al.* (Ref. 11). For the purpose of comparison, the energy reference (zero of energy) was set such that the highest valence-band DOS peak coincides with the position of the corresponding peak in the data from the previous UPS experiment by Ueda *et al.* (Ref. 11).

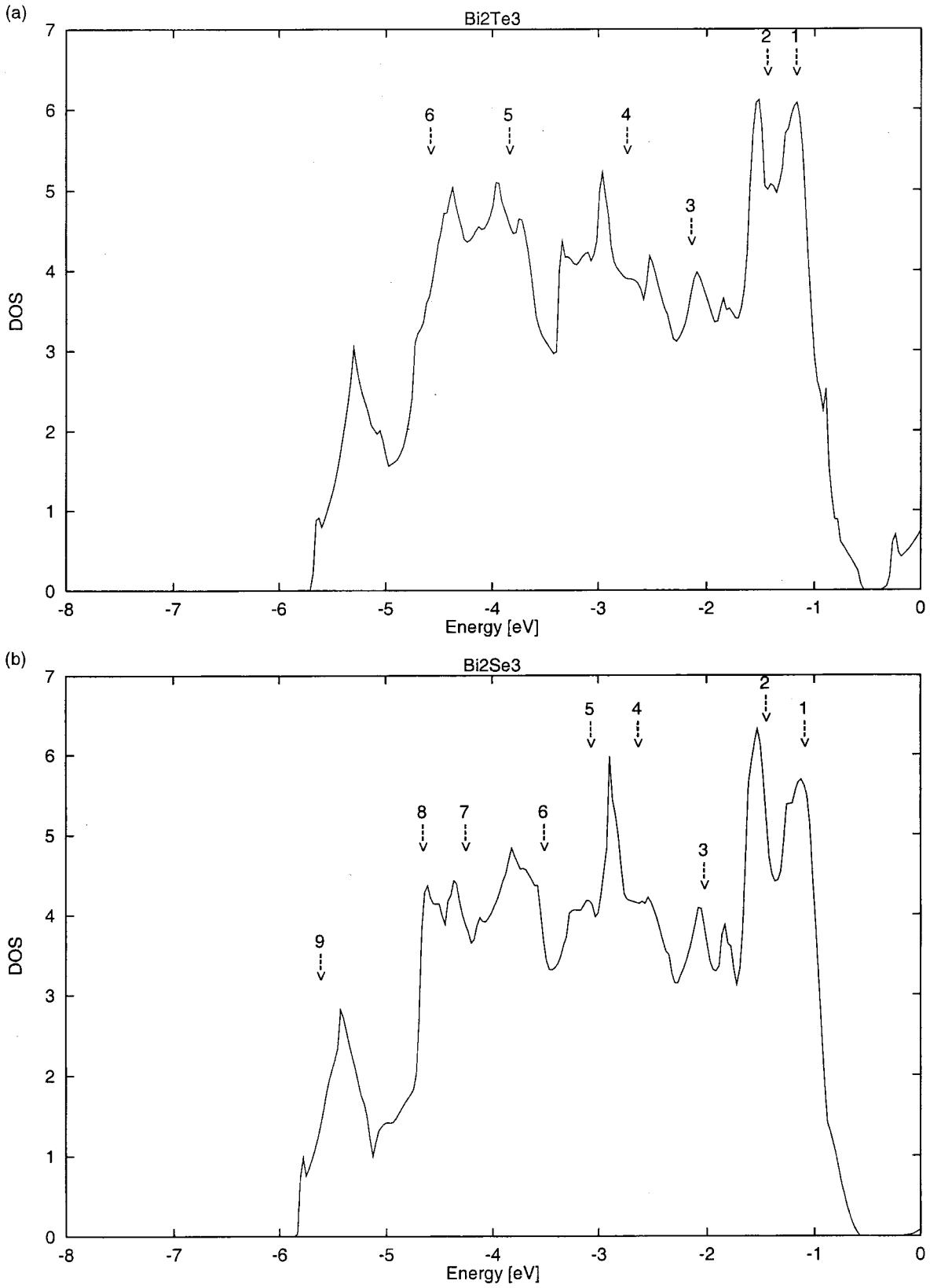

FIG. 9. Total density of states of (a) Bi_2Te_3 and (b) Bi_2Se_3. The arrows indicate the positions of the photoemission peaks seen in the present work. For the purpose of comparison, the energy reference (zero of energy) was set such that the highest valence-band DOS peak coincides with the position of the corresponding peak in the data from our most recent experiment.

mento *et al.*,[12] they show fewer details than does our present PES study, due to the inferior energy resolution and the use of a single-photon energy.

IV. COMPARISON OF THEORY TO PHOTOEMISSION EXPERIMENTS

The theoretical DOS for the four systems are shown in Figs. 8(a)–8(d). An energy resolution of 0.02 eV was used in the calculated DOS. For the purpose of comparison with experiments, the energy reference was set such that the highest-energy valence-band peak coincided with the highest-energy valence band peak seen in the spectra by Ueda *et al.*[11] As discussed previously, the same has been done with our most current experimental spectra.

These systems are all narrow-gap semiconductors, the gap being smallest in Bi_2Te_3 and largest in Bi_2S_3. The calculated DOS of Bi_2Se_3 and Bi_2Te_3 are similar to the earlier LMTO-ASA calculations.[6] While the positions of the peaks in the calculated DOS are about the same, the relative heights of the peaks differ between these two calculations. The main difference is that in the present LAPW calculations the highest-energy valence-band peak consists actually of two peaks separated by about 0.3 eV whereas only one peak was seen in the LMTO-ASA calculation in the same energy range.[6]

As discussed earlier, matrix element effects in the PES spectra make a direct comparison of the complete spectra with the calculated DOS less meaningful. Instead we will focus on comparing the peak positions. The arrows in Fig. 8 show the positions of the dominant experimental peaks found by Ueda *et al.*[11] They are labeled c1–c3 in the conduction band and v1–vn ($n=3$ for Bi_2Te_3, $n=5$ for Bi_2Se_3 and Bi_2Te_2Se, and $n=4$ for Bi_2S_3) in the valence band, v1 and c1 being closest to E_F. The arrows in Fig. 9 show the positions of the dominant experimental peaks found in our latest measurement. The positions of the major peaks in Bi_2Te_3, Bi_2Te_2Se, Bi_2Se_3, and Bi_2S_3 are given in Tables I(a)–I(d). The first columns give the peak positions for both the valence and conduction bands by Debies and Rabalais,[10] Ueda *et al.*,[11] Nascimento *et al.*,[12] and this work. The last column (with the heading "DOS") presents the positions of the peaks obtained from our electronic structure calculations.

Let us discuss some general aspects of the comparison between the photoemission spectra and the calculated DOS. The width of the valence band in the DOS for all four systems is about 5–5.5 eV (Fig. 8). While the background tends to obscure the edge of the band, a sharp drop in the photoemission spectra is seen around 5–5.5 eV (Figs. 5 and 6). In Bi_2S_3 the width of the spectra for both the DOS (Fig. 8) and the photoemission spectrum (Fig. 7) are about 5–5.5 eV, although there is a shift down in energy of the valence-band top so that the valence bands terminate close to 7 eV below the designated Fermi level.[11]

The most important and robust feature we see in the calculated DOS in all four compounds is the double peak structure near the top of the valence band. The separation of these peaks in the DOS is found to be 0.3 eV in Bi_2Te_3, 0.4 eV in Bi_2Te_2Se, 0.4 eV in Bi_2Se_3, and 0.7 eV in Bi_2S_3. An orbital analysis of these peaks shows that the peak closest to the Fermi level has nearly equal amounts of Te1 p and Te2 (Se2) p character in Bi_2Te_3 (Bi_2Te_2Se). The lower peak has about 10% more Te2 p character than Te1 p character in Bi_2Te_3 and 25% more Se2 p character than Te1 character in Bi_2Te_2Se. (The Bi p character of both peaks is only about 20%–25% that of the Te1 p or Te2 p character.) Therefore, this peak changes shape when Se is placed in the Te2 position of Bi_2Te_3 to form Bi_2Te_2Se. In Bi_2Se_3 both peaks have about 25%–30% more Se1 p character than Se2 p character.

The double peak structure was not resolved in the work of Debies and Rabalais[10] or Nascimento *et al.*[12] due to poor

TABLE I. Comparison of photoemission and calculated DOS peaks for (a) Bi_2Te_3, (b) Bi_2Te_2Se, (c) Bi_2Se_3, and (d) Bi_2S_3. For (a)–(c) the theoretical reference energies are chosen such that the highest valence-band peak positions coincided with experiment (Ref. 11). For (d), the theoretical reference energies are chosen so that the top two calculated valence band peaks lie equidistant from the highest experimental peak in the experiment (Ref. 11).

(a)

Bi_2Te_3			
Valence band (Debies and Rabalais) (eV)	Valence band (Ueda *et al.*) (eV)	Valence band (this work) (eV)	DOS (eV)
−1.2	−1.1	−1.10	−1.1
	−1.6	−1.37	−1.4
		−2.07	−2.0
		−2.66	−2.5
−3.4	−3.5	−3.77	−3.8
		−4.51	−4.2
			−5.2
	Conduction band (Ueda *et al.*) (eV)		
	0.7		0.5
	1.7		1.0
	3.4		2.9

(b)

Bi_2Te_2Se	
Valence band (Ueda *et al.*) (eV)	DOS (eV)
−1.1	−1.1
−1.6	−1.5
	−2.0
−2.9	
−3.5	−3.9
−4.2	−4.6
−5.3	
Conduction band (Ueda *et al.*) (eV)	
0.7	0.7
	1.4
	1.8
2.5	3.1
3.7	3.7

TABLE I. (*Continued*.)

(c)

Bi_2Se_3

Valence band (Nascimento *et al.*) (eV)	Valence band (Debies and Rabalais) (eV)	Valence band (Ueda *et al.*) (eV)	Valence band (this work) (eV)	DOS (eV)
		−1.1	−1.10	−1.1
	−1.6	−1.6	−1.46	−1.5
−2.1			−2.03	−2.1
			−2.64	−2.9
			−3.08	
		−3.3	−3.52	−3.8
−4.4	−4.4	−4.2	−4.26	−4.4
			−4.66	−4.6
		−5.4	−5.62	−5.4

Conduction band (Nascimento *et al.*) (eV)	Conduction band (Ueda *et al.*) (eV)	
	1.0	0.9
		1.4
	2.5	2.1
3.5	3.8	3.4

(d)

Bi_2S_3

Valence band (Debies and Rabalais) (eV)	Valence band (Ueda *et al.*) (eV)	DOS (eV)
−2.2	−2.2	−1.9
		−2.6
	−3.4	−3.5
		−3.8
		−4.1
	−4.6	−4.5
		−5.0
	−5.7	−5.7
		−6.7

Conduction band (Ueda *et al.*) (eV)	
	0.4
0.9	0.9
	1.5
2.5	2.7
4.0	4.1

energy resolutions. The separation between these peaks in the ultraviolet photoemission spectroscopy (UPS) study by Ueda *et al.*[11] (with resolution of 0.2 eV) was found to be 0.5 eV in Bi_2Te_3, Bi_2Te_2Se, and Bi_2Se_3. Only one peak was seen in Bi_2S_3. It is possible that one of these peaks was not seen due to matrix element effects. Our present PES studies, with a resolution of 0.08 eV, find separations of 0.27 eV in Bi_2Te_3 and 0.36 eV in Bi_2Se_3, much closer to the separation found in the calculated DOS.

With improved experimental resolution, more peaks are found in the photoemission spectrum that agree with more features in the calculated DOS (Fig. 9). Good agreement is found for peaks 7–9 in Bi_2Se_3 and for peaks 5 and 6 in Bi_2Te_3. No peak was found near 5.2 eV in the PES spectra to correspond with the lowest-lying peak in the DOS Bi_2Te_3 while two peaks were found at −2.64 and −3.08 eV, equidistant from the calculated DOS peak at −2.9 eV. Although the energy dependence of matrix elements can move the positions of the peaks obtained in the DOS, we find overall good agreement between the DOS peak positions and the

PES peak positions.

In Bi_2Te_2Se and Bi_2S_3, which had been studied earlier by Ueda *et al.*,[11] the agreement is not as good due to the lower-energy resolution and because the spectrum was taken only at one photon energy. While the number of peaks seen in the theoretical DOS of Bi_2Te_2Se is nearly two times the number seen in the photoemission experiment, the experimentally observed peak positions agree fairly well with the peaks found in the DOS. The large number of peaks seen in the DOS of Bi_2S_3 makes any comparison difficult at best, especially for the resolution in this experiment.[11] Improved experimental resolution and taking spectra at several different energies do lead to better agreement between the positions of the photoemission peaks and the peaks found in the calculated DOS.

V. SUMMARY AND CONCLUSIONS

In summary, the *ab initio* FLAPW electronic structure calculations of Bi_2S_3, Bi_2Se_3, Bi_2Te_2Se, and Bi_2Te_3 show that these materials are narrow-gap semiconductors and the gap structure is strongly determined by spin-orbit interaction. The agreement between the theoretical (calculated by DFT GGA) and experimental gaps is very good, unlike that of many other semiconductors (Si, Ge, and groups IV, III–V, II–VI).[26] In the four systems studied, the calculated DFT band structure over a broad energy range is also remarkably good. The reason for this may be that the general features of the band structure arise from the strong hybridization of the Bi $6p$ and X np ($n=3$ for S, $n=4$ for Se, and $n=5$ for Te) orbitals.

In addition to the gap structure, good overall agreement was also found between the positions of the peaks in the DOS and both the new PES data as well as earlier PES measurements.[11] In Bi_2Te_3 and Bi_2Se_3, the valence-band peak positions found in the current experiment, which had an energy resolution of 0.08 eV (compared to 0.2 eV in the previous study[11]), agreed very well with the calculated peak positions (with a resolution of 0.02 eV). In addition, our PES study clearly illustrates the benefits of using a synchrotron photon source over a single-line light source; the ability to scan at multiple photon energies allows one to identify several peaks which would be otherwise indistinguishable or absent. With improved energy resolution of the experiment and by incorporating matrix element effects into the calculated DOS, a better agreement should be obtained for Bi_2S_3 and Bi_2Te_2Se as well.

ACKNOWLEDGMENTS

We thank Dr. Yoshifumi Ueda for a copy of photoemission and inverse-photoemission data, which has been reproduced here. We also thank Dr. Mercouri Kanatzidis and Dr. Duck-Young Chung for providing the Bi_2Te_3 and Bi_2Se_3 samples used in the photoemission experiment. The angle-integrated experiment was conducted at the Synchrotron Radiation Center, University of Wisconsin, Madison, and was supported by the National Science Foundation (NSF) Award No. DMR9531009. Ames Laboratory is operated for the U.S. DOE by Iowa State University under Contract No. W-7405-ENNG-82. The experimental work was supported by the Center for Fundamental Materials Research (CFMR) at Michigan State University and by the NSF Award No. DMR9801776. The theoretical work was supported by DARPA Grant No. DAAG55-97-1-0184.

[1] *Thermoelectric Materials 2000–The Next Generation Materials for Small-Scale Refrigeration and Power Generation Applications*, edited by T. M. Tritt, G. S. Nolas, G. Mahan, M. G. Kanatzidis, and D. Mandrus, Mater. Res. Soc. Symp. Proc. No. 626 (Materials Research Society, Pittsburgh 2001).

[2] H. J. Goldsmid, *Thermoelectric Refrigeration* (Plenum, New York, 1964); A. F. Ioffe, *Thermoelements and Thermoelectric Cooling* (Infosearch, London, 1957); D. M. Rowe, *CRC Handbook of Thermoelectrics* (Chemical Rubber, Boca Raton, Florida, 1995).

[3] B. Chen, C. Uher, L. Iordanidis, and M. G. Kanatzidis, Chem. Mater. **9**, 1655 (1997).

[4] J. M. Schoijet, Sol. Energy Mater. **1**, 43 (1979).

[5] E. V. Oleshko and V. N. Korolyshin, Fiz. Tekh. Poluprovodn. **19**, 1839 (1985) [Sov. Phys. Semicond. **19**, 1130 (1985)].

[6] S. K. Mishra, S. Satpathy, and O. Jepsen, J. Phys.: Condens. Matter **91**, 461 (1997).

[7] P. M. Lee and L. Pincherlee, Proc. Phys. Soc. London **81**, 462 (1963); F. Borghese and E. Donato, Nuovo Cimento Soc. Ital. Fis., **53B**, 283 (1968); Shin-ichi Katsuki, J. Phys. Soc. Jpn. **26**, 58 (1969); R. Togei and G. R. Miller, J. Phys. Chem. Solids Suppl. **32**, 349 (1971); E. V. Oleeshko and V. N. Koryshin, Fiz. Tverd. Tela (Leningrad) **27**, 2856 (1985) [Sov. Phys. Solid State **27**, 1723 (1985)]; G. A. Thomas, D. H. Rapke, R. B. Van Dover, L. F. Mattheis, W. A. Surden, L. F. Schneemaper, and J. V. Waszczak, Phys. Rev. B **46**, 1553 (1992).

[8] P. Larson, S. D. Mahanti, and M. G. Kanatzidis, Phys. Rev. B **61**, 8162 (2000).

[9] S. Hufner, *Photoelectron Spectroscopy* (Springer, New York, 1995).

[10] T. P. Debies and J. W. Rabalais, Chem. Phys. **20**, 277 (1977).

[11] Y. Ueda, A. Furuta, H. Okuda, M. Nakatake, H. Sato, H. Namatame, and M. Taniguchi, J. Electron Spectrosc. Relat. Phenom. **103**, 677 (1999).

[12] V. B. Nascimento, V. E. de Carvalho, R. Paniago, E. A. Soares, L. O. Ladeira, and H. D. Pfannes, J. Electron Spectrosc. Relat. Phenom. **104**, 99 (1999).

[13] D. Singh, *Planewaves, Pseudopotentials, and the LAPW Method* (Kluwer Academic, Boston, 1994).

[14] P. Hohenberg and W. Kohn, Phys. Rev. B **163**, B864 (1964); W. Kohn and L. Sham, *ibid.* **140**, A1133 (1965).

[15] J. P. Perdew, K. Burke, and M. Ernzerhof, Phys. Rev. Lett. **77**, 3865 (1996).

[16] P. Blaha, K. Schwarz, and J. Luitz, computer code WIEN97 (Vi-

enna University of Technology, Vienna, 1997).
[17] D. Koelling and B. Harmon, J. Phys. C **13**, 6147 (1980).
[18] R. W. G. Wyckoff, *Crystal Structures* (Krieger, Melbourne, FL, 1986), Vol. 2.
[19] B. Schroeder, A. Von Middendorf, H. Kohler, and G. Landwehr, Phys. Status Solidi B **59**, 561 (1973).
[20] V. A. Davidenko, J. Phys. (Moscow) **4**, 170 (1941); E. Mooser and W. B. Pearson, Phys. Rev. **101**, 492 (1956); J. Black, E. M. Conwell, L. Seigle, and C. W. Spencer, J. Phys. Chem. Solids **2**, 240 (1957).
[21] H. Kohler, Phys. Status Solidi B **58**, 91 (1973).
[22] H. Kohler and J. Hartmann, Phys. Status Solidi B **63**, 171 (1974).
[23] R. S. Erofeev and E. I. Shcherbina, Inorg. Mater. (Transl. of Neorg. Mater.) **18**, 1546 (1982).
[24] V. A. Greanya, W. C. Tonjes, Rong Liu, C. G. Olson, D.-Y. Chung, and M. G. Kanatzidis, Phys. Rev. B **62**, 16 425 (2000).
[25] H. Mizoguchi, H. Hosono, N. Ueda, and H. Kawazoe, J. Appl. Phys. **78**, 1376 (1995); J. Lukose and B. Pradeep, Solid State Commun. **78**, 535 (1991).
[26] Wilfried G. Aulbur, Lars Jonsson, and John W. Wilkins, in *Solid State Physics*, edited by H. Ehrenreich and F. Spaepen (Academic, Orlando, 2000), Vol. 54, p. 1.